ARTMS: Enabling Autonomous Distributed Angles-Only Orbit Estimation for Spacecraft Swarms

Adam W. Koenig[1], Justin Kruger[2], Joshua Sullivan[3], and Simone D'Amico[4]

***Abstract*— This paper presents the design and expected performance of the Absolute and Relative Trajectory Measurement System (ARTMS), which is a software payload that provides autonomous, distributed navigation capability for spacecraft swarms in deep-space using low-cost optical sensors. This payload combines key innovations of recent works by the authors to overcome four major shortcomings of previous flight demonstrations of angles-only navigation: 1) lack of autonomy and reliance on accurate a-priori information from the ground, 2) inability to accommodate multiple observers and targets, 3) reliance on frequent translational maneuvers to improve observability, and 4) inability to estimate the absolute orbit of the observer satellite. The first innovation is a target detection and tracking algorithm that robustly identifies multiple targets across images from a single camera without requiring a-priori relative orbit knowledge. Second, a new batch orbit determination algorithm based on relative orbital elements provides estimates of the orbits of all spacecraft in the local swarm using a one-dimensional sampling scheme to accurately resolve the range to each target. Third, a sequential orbit determination algorithm based on the unscented Kalman filter continuously estimates the orbits and auxiliary parameters of the local swarm by seamlessly fusing measurements from multiple observers exchanged over an inter-satellite link. Functionality and performance of ARTMS are demonstrated through a sensor-in-the-loop simulation of fully autonomous angles-only orbit estimation using two observers in low earth orbit with no simplifying assumptions, which has never before been shown in literature. The results demonstrate that the ARTMS payload meets key needs of future deep space missions by providing autonomous, robust, and scalable absolute and relative navigation capabilities using low-cost hardware with minimal reliance on maneuvers and a-priori information.**

I. INTRODUCTION

While formation flying and spacecraft swarm technologies have received a great deal of attention in recent literature, the majority of missions to date have been deployed in earth orbit [1], [2], [3], [4]. Accordingly, the navigation systems for these missions assume the availability of external metrologies such as GNSS signals and frequent contact with the ground. To enable deployment of satellite swarms and formations in deep space, it is necessary to develop new self-contained navigation systems characterized by a high degree of autonomy and robustness. It is also desirable to minimize the technical and financial budgets required for associated hardware. Angles-only navigation is a promising technology for deep space missions because vision-based sensors (VBS) are already ubiquitous on modern spacecraft in the form of star trackers. These sensors are passive and inexpensive with a high dynamic range (hundreds of kilometers or more) and require minimal mass, volume, and power budgets [5]. If the spacecraft are equipped with an inter-satellite link (ISL), which is already required for any form of cooperative navigation, measurements from multiple observers can be fused to improve performance. Accordingly, angles-only navigation will generally require no additional hardware even when used on small and inexpensive spacecraft.

Angles-only navigation has been tested on orbit, most notably in the ARGON experiment in 2012 [6] and in the AVANTI experiment in 2016 [7], [8], [9]. However, these demonstrations are characterized by four major deficiencies that must be overcome to meet the needs of future missions. These limitations are: 1) inability to accommodate multiple observers and multiple targets, 2) lack of autonomy and reliance on accurate a-priori relative orbit information from the ground, 3) reliance on external knowledge of the observer's absolute orbit (e.g. from a GNSS receiver), and 4) reliance on frequent translational maneuvers to resolve the weakly observable inter-spacecraft separation. Other authors have produced more sophisticated algorithms for individual navigation tasks such as target detection and tracking [10], initial relative orbit determination [11], [12], and sequential filtering [13], but these approaches each suffer from a subset of the aforementioned limitations, or are otherwise unsuitable for the space-based angles-only navigation context and its associated constraints.

To overcome these limitations and meet the navigation needs of future swarming missions in deep space, this paper presents a high-level overview of the Absolute and Relative Trajectory Measurement System (ARTMS), which is a self-contained software payload first proposed in [14] that provides distributed, autonomous navigation capability for spacecraft swarms in any planetary orbit regime. This payload will be tested on orbit in the Starling Formation-flying Optical eXperiment (StarFOX), which is part of the Starling1 mission in development at NASA Ames Research Center [15]. The only hardware requirements posed on a spacecraft with ARTMS are that it must have a VBS and an ISL. If available, an absolute orbit metrology system such

*This work was supported by the NASA Small Spacecraft Technology Program (cooperative agreement number 80NSSC18M0058) for contribution to the Starling-1/StarFOX efforts.

[1]Adam W. Koenig is a Postdoctoral Scholar in the Space Rendezvous Laboratory, Stanford University, Stanford, CA 94305, USA awkoenig@stanford.edu

[2]Justin Kruger is a Ph.D. candidate in the Space Rendezvous Laboratory, Stanford University, Stanford, CA 94305, USA jjkruger@stanford.edu

[3]Joshua Sullivan is a Guidance, Navigation, and Control Engineer at Astranis, San Francisco, CA 94107, USA jasulliv@stanford.edu

[4]Simone D'Amico is the PI of the Space Rendezvous Laboratory, Stanford University, Stanford, CA 94305, USA damicos@stanford.edu

as a GNSS receiver can be included to improve navigation performance. ARTMS is divided into three modules that are based on algorithms recently developed by the authors: image processing (IMP) [16], batch orbit determination (BOD) [17], and sequential orbit determination (SOD) [18]. Each module is developed to operate with minimal a-priori information and exploit absolute and relative state knowledge as it becomes available. Overall, the ARTMS payload provides estimates of the orbits of the host spacecraft and each target detected by the onboard sensor as long as each observer is provided with an estimate of its orbit at a single epoch.

After this introduction, key modeling assumptions are provided in Section II and a high-level overview of the payload and its constituent modules is provided in Sections III-VI. Next, Section VII presents a high-fidelity sensor-in-the-loop simulation that exercises the autonomous navigation capability of the ARTMS payload on two cooperative observer satellites in low earth orbit (LEO). The included sensor is a Nano Star Tracker by Blue Canyon Technologies [5] that is stimulated by the Space Rendezvous Laboratory's Optical Stimulator (OS) testbed [19]. In this scenario, each observer is provided with a single estimate of its absolute orbit, which it uses to track targets, compute an initial estimate of the swarm state using measurements from the onboard sensor, and then sequentially refine the state estimate using measurements from both observers. This scenario is representative of a planned test in the StarFOX experiment [15] and future deep space missions, which will not have access to external metrologies such as GNSS. Finally, conclusions are summarized in Section VIII.

II. MODELING PRELIMINARIES

Because angles-only navigation is known to be characterized by weak observability [20], proper selection of the state parameterization is particularly important to maximize accuracy of state estimates and robustness to errors in a-priori information. Specifically, the state definition should be selected to meet two objectives: 1) separate weakly and strongly observable terms to enable use of separate estimation techniques and 2) maximize accuracy and computational efficiency of orbit propagation. To meet both of these objectives, the swarm state is defined using quasi-nonsingular absolute and relative orbital elements. The absolute orbit α is defined as

$$\alpha = \begin{pmatrix} a \\ e_x \\ e_y \\ i \\ \Omega \\ u \end{pmatrix} = \begin{pmatrix} a \\ e\cos(\omega) \\ e\sin(\omega) \\ i \\ \Omega \\ \omega + M \end{pmatrix} \tag{1}$$

where a, e, i, Ω, ω, and M are the canonical Keplerian orbit elements including the semimajor axis, eccentricity, inclination, right ascension of the ascending node (RAAN), argument of periapsis, and mean anomaly, respectively. The relative orbit of each target detected by the onboard sensor, denoted $\delta\alpha$, is described by the ROE adopted by D'Amico [21]. Each of these ROE is function of the orbit elements of the target (denoted by subscript t) and observer (denoted by subscript o) as given by

$$\delta\alpha = \begin{pmatrix} \delta a \\ \delta\lambda \\ \delta e_x \\ \delta e_y \\ \delta i_x \\ \delta i_y \end{pmatrix} = \begin{pmatrix} (a_t - a_o)/a_o \\ u_t - u_o + \cos(i_o)(\Omega_t - \Omega_o) \\ e_{x,t} - e_{x,o} \\ e_{y,t} - e_{y,o} \\ i_t - i_o \\ \sin(i_o)(\Omega_t - \Omega_o) \end{pmatrix}. \tag{2}$$

These state definitions have been well-studied in literature, resulting in development of several accurate analytical dynamics models for earth orbit regimes (e.g. [22] and [23]). Also, these states are slowly varying and enable accurate numerical integration using Gauss's variational equations with large time steps [24]. More importantly, the weakly observable range to each target is primarily captured by the $\delta\lambda$ term in most formation-flying relative motion geometries. Additionally, it has been shown that the semimajor axis of the observer's orbit is strongly observable using bearing angle measurements to a single target [17]. Combined, these properties enable accurate and computationally efficient estimation algorithms with minimal reliance on a-priori information.

III. ARTMS PAYLOAD OVERVIEW

To simplify subsequent discussions, the following terminologies are adopted in this paper. The "observer" refers to the spacecraft hosting the instance of the ARTMS payload being discussed. A "remote observer" is another spacecraft hosting an ARTMS payload that is providing measurements over the ISL. The "local swarm" includes the observer and all "targets", which are spacecraft or resident space objects detected by the onboard VBS. In most scenarios of interest, the targets will include one or more remote observers.

A high-level overview of the ARTMS software payload is shown in Figure 1 including modules (green), external systems (gray), and exchanged data (blue). ARTMS is divided into three main modules: IMP, BOD, and SOD. The payload interfaces with the onboard VBS, the ISL, the ground segment, and (if available) an onboard GNSS receiver. The VBS provides time-tagged raw images to the payload. The ground segment provides telecommands as well as maneuver plans and orbit estimates for each observer in the swarm and receives telemetry from each instance of ARTMS. The ISL communicates orbit estimates and angles measurements between all observers in the swarm. If the spacecraft is equipped with a GNSS receiver, it provides the payload with position/velocity/time (PVT) measurements to replace less timely orbit estimates from the ground.

The IMP module converts images from the VBS to time-tagged batches of bearing angles to each detected target, which are provided to the BOD and SOD modules. The module requires only a coarse estimate of the observer's orbit, but uses relative orbit information from SOD (when available) to reduce computation cost. The BOD module computes orbit estimates for all spacecraft in the local swarm

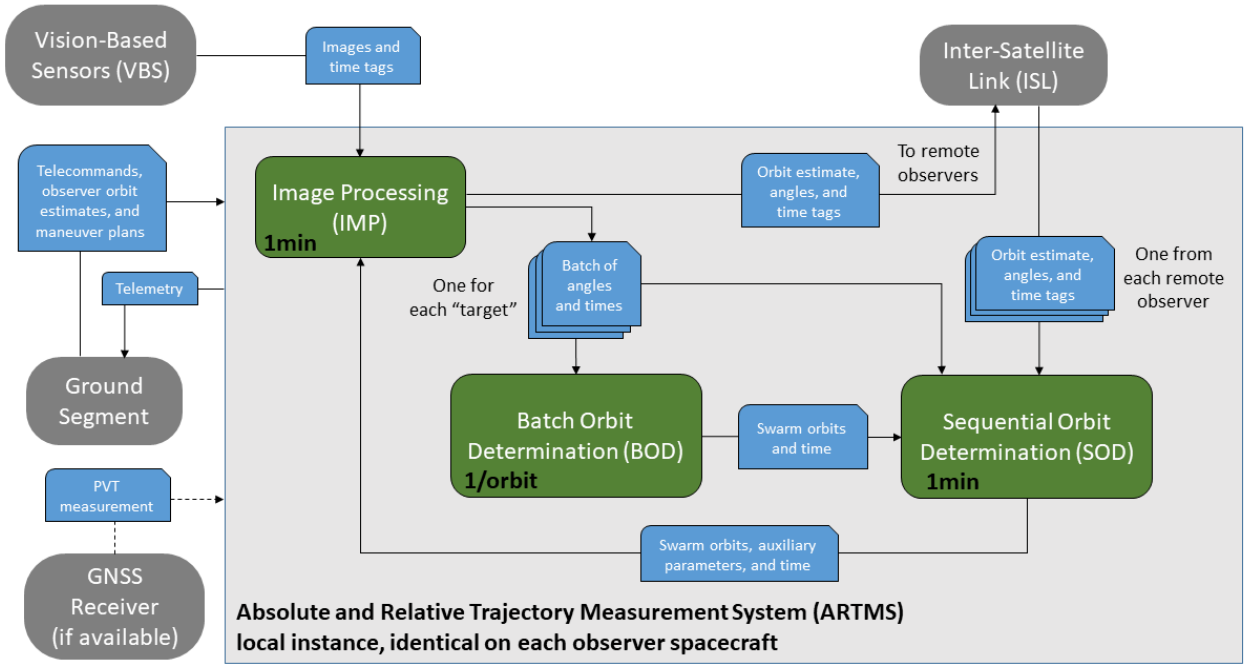

Fig. 1. Architecture of ARTMS payload updated from [14] including external systems (gray), software modules (green), and exchanged data (blue).

using only a time-tagged estimate of the observer's orbit and batches of bearing angles to each target provided by IMP. This swarm estimate is provided to SOD for both initialization and fault detection. Finally, the SOD module uses the swarm estimate from BOD to initialize a UKF that continuously fuses measurements from the IMP module and remote observers to estimate the orbits of all spacecraft in the local swarm as well as auxiliary parameters (e.g. ballistic coefficients or differential clock offsets). These estimates are provided to the ground and to the IMP module to reduce computation cost of image processing. More detailed descriptions of each ARTMS module are provided in the following sections.

IV. IMAGE PROCESSING

The objective of the IMP module is to produce batches of time-tagged bearing angle measurements to each target using a coarse estimate of the observer's orbit and images provided by the onboard VBS. This is accomplished in two phases. First, each incoming image is processed and reduced to a set of inertial bearing angles that may correspond to resident space objects. Second, these candidate bearing angles are used to track known targets and detect new targets using an approach inspired by multi-hypothesis tracking (MHT) [10].

The first phase of IMP uses a set of well-known algorithms that have extensive flight heritage. First, a centroiding algorithm is used to simplify the raw image into a list of pixel cluster centroids. Second, these centroids are converted to unit vectors in the sensor frame using the calibrated sensor model. Next, the pyramid star identification algorithm [25] is applied to remove stellar objects (SO) from the list of pointing vectors. Uncatalogued SO are detected by considering objects with unchanging inertial unit vectors between images. Similarly, camera hotspots are removed by considering objects with unchanging pixel coordinates. The VBS attitude is computed from the pointing vectors to identified stars in the inertial and sensor frames using the q-method [26]. The remaining minimalistic set of inertial unit vectors (and corresponding bearing angles in the sensor frame) likely correspond to known targets or other unknown objects in the field of view (FOV).

In the second phase, these measurement candidates must be consistently assigned to new targets or targets that are currently being tracked without requiring a-priori relative orbit knowledge. To accomplish this, the IMP module employs the new Spacecraft Angles-only MUltitarget tracking System (SAMUS) [27], which has only two key requirements: 1) a coarse estimate of the observer's absolute orbit must be provided, and 2) targets must not perform translational maneuvers during the tracking period. SAMUS is valid for orbits of arbitrary eccentricity and has been specifically designed to meet the constraints of risk-averse angles-only navigation in space, i.e. to achieve close to 100% measurement assignment precision with low measurement frequencies and limited computational resources.

SAMUS applies the core concept of MHT in that as measurements arrive, many simultaneous hypotheses are maintained as to how they can be associated into target tracks. The algorithm converges towards the correct hypothesis over time, with the aim of improved robustness. MHT is chosen

as a basis because it is mature and demonstrably accurate, with its primary disadvantage being the need to frequently and heuristically trim hypotheses for real-time computation [28]. To overcome this, SAMUS applies domain-specific knowledge to develop precise trimming criteria.

D'Amico defines a mapping between the ROE and a target's curvilinear position vector δr in the observer's radial/tangential/normal (RTN) reference frame [21], as

$$\delta r = \begin{bmatrix} \delta r_R \\ \delta r_T \\ \delta r_N \end{bmatrix} = a_o \begin{bmatrix} \delta a - \delta e \cos(u_o - \phi) \\ \delta \lambda + 2\delta e \sin(u_o - \phi) \\ \delta i \sin(u_o - \theta) \end{bmatrix} \tag{3}$$

This form applies to near-circular orbits, and Sullivan provides a more general mapping for eccentric orbits in [29]. Note that above, u_o is the only quickly-varying term, while all other terms vary slowly in the presence of perturbations and are effectively constant on timescales of image-to-image tracking. Thus, target motion is described by periodic, parametric functions with known form. Even if the specific ROE in Equation 3 are unknown, its form provides expectations regarding target motion that can be leveraged.

Perturbing forces, such as spherical harmonic gravity and atmospheric drag, can disturb the form of Equation 3. However, in angles-only scenarios of interest, swarm members are relatively close together in inertial space and are affected similarly by perturbations. By synchronously differencing the measurements of different targets in bearing angle space – in essence, using one track as a virtual, moving origin for another – perturbation effects are approximately cancelled between targets, recovering motion as per Equation 3.

Given a set of past bearing angles measurements in a track and corresponding estimates of the observer's absolute orbit, Equation 3 can be rearranged into a pair of separable linear systems in azimuth and elevation [27]. The unknown terms, which are scaled ROE equivalents in bearing angle space, can be solved for via least squares as long as at least three past measurements exist. Subsequently, upcoming measurements in a new image can be predicted using the fitted model and the observer's orbit estimate.

To assess which hypotheses are physically reasonable, SAMUS applies a set of kinematic rules derived from the parametric motion model. Only tracks which pass all rules are propagated. Briefly, the rules are summarised as:

1) Track velocities must be below a set maximum
2) Track velocities must be consistent over time
3) Tracks should generally not feature acute angles
4) Tracks should turn in a consistent direction
5) New data must be close to the predicted measurement

Their application greatly increases efficiency of MHT by preventing formation of unlikely tracks. Mathematical definitions for these rules are provided in [27]. When multiple tracks pass all rules, SAMUS scores propagated tracks via ten criteria which assess how well each fulfills the expectations of Equation 3 and their past motion. In contrast to traditional MHT methods – which often rely on a single Mahalanobis distance metric for scoring – SAMUS aims to be more robust. Often, target tracks intersect or are in close proximity in the image plane, or motion between images is on the order of VBS noise. A single scoring metric is therefore not robust. By using a larger set of metrics, consensus supports the correct choice over time, even if some temporarily support incorrect hypotheses. Additionally, scoring does not require probabilistic estimates of false alarm densities or target decay rates, which are not easily obtainable for spacecraft.

To initialize new tracks, SAMUS employs the Density-Based Spatial Clustering of Applications with Noise (DBSCAN) algorithm [30]. DBSCAN clusters require $\geq n_D$ points within small radius ε_D. Because targets are in similar orbits to observers, their velocities compared to other objects in the FOV are low. Previously untracked targets are initialized by applying DBSCAN to the merged set of unidentified measurements from the past several images, and applying the SAMUS kinematic rules to found clusters.

Finally, given the use of visual measurements, tracking is often interrupted by orbit eclipse periods. To connect shorter tracks on either side of an eclipse, the aforementioned linear system fit is computed for every possible set of paired tracks. The combination of compatible pairs which produces the least fitting residuals is chosen as output.

SAMUS is also able to cooperate with SOD and apply target state knowledge. If available, target state estimates from SOD are propagated into the current epoch to provide predicted track measurements. The kinematic rules are replaced by a validity region around the predicted measurement, computed via an unscented transform of the target state covariance. The Mahalanobis distance between predicted and assigned measurement is employed for track scoring. Figure 2 presents an overview of core SAMUS operations, with further detail provided in [27].

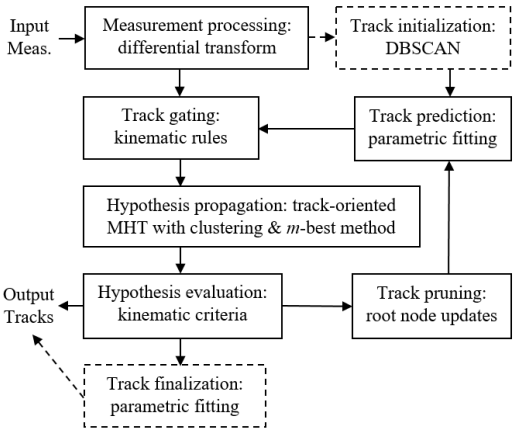

Fig. 2. SAMUS algorithm summary and core sequence of operations. Dashed lines denote steps that only occur at relevant epochs.

V. BATCH ORBIT DETERMINATION

The BOD module must be able to produce orbit estimates for the local swarm with sufficient accuracy to initialize the SOD module using only a coarse estimate of the observer's

orbit and batches of bearing angles to each target from the onboard sensor. For simplicity, it is assumed that targets do not perform any translational maneuvers between the epochs of the first and last measurement of the provided measurement batch for each target. State estimation is accomplished using an algorithm based on [17] that sequentially estimates the relative orbits of each target while simultaneously refining the estimate of the semimajor axis of the observer's orbit. When used in LEO, the algorithm uses a fully analytical dynamics model including the earth oblateness J_2 perturbation developed by the authors to minimize computation cost [22]. For each target, the estimation process is a four-step procedure that was inspired by the work of Ardaens [12]. First a one-dimensional family of state estimates is computed for user-specified values of $\delta\lambda$ (selected based on system limitations such as sensitivity of the VBS) using iterative batch least squares refinement until either 1) a user-specified iteration limit is reached, or 2) the step size is smaller than a user-specified convergence threshold. Second, the final state estimate is selected as the candidate state estimate with the smallest measurement residuals. A conceptual illustration of the BOD state selection process for a single target is shown in Figure 3 including specified values of $\delta\lambda$ and measurement residuals for selected and rejected state estimates. Third, the

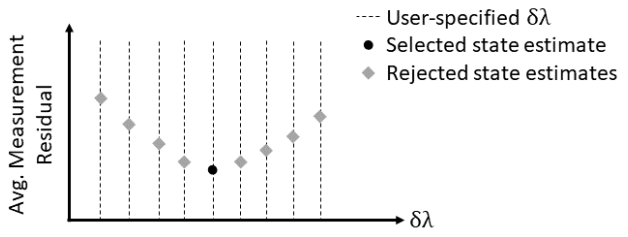

Fig. 3. Conceptual illustration of converged measurement residuals for rejected (gray) and selected (black) state estimates at specified values of $\delta\lambda$ for a single target in the BOD module.

measurement noise matrix for each measurement (denoted $\mathbf{R}_{sensor}$) is estimated using the measurement residuals corresponding to the final state estimate. Fourth, the covariance for estimated state components $\mathbf{P}_{est}$ is computed as given by

$$\mathbf{P}_{est} = \mathbf{Y}^*_{est}(N\mathbf{R}_{sensor} + \mathbf{Y}_{prior}\mathbf{P}_{prior}\mathbf{Y}^T_{prior})\mathbf{Y}^{*T}_{est} \qquad (4)$$

where $\mathbf{Y}^*_{est}$ is the pseudoinverse of the measurement sensitivity matrix for estimated state components, $\mathbf{Y}_{prior}$ is the measurement sensitivity matrix for a-priori information (orbit elements other than the semimajor axis, ballistic coefficients, sensor biases, etc.), $\mathbf{P}_{prior}$ is the uncertainty of the a-priori information, and N is the number of provided bearing angle measurements. This formulation allows the BOD module to seamlessly transition between domains where uncertainty is driven by sensor performance and by errors in the a-priori information. Finally, the ROE estimates for each target are appended to the refined estimate of the observer's absolute orbit, forming a complete estimate of the state of the local swarm.

It was demonstrated in [17] that this estimation approach can provide relative orbit estimates with range errors of less than 20% (3-σ) in the presence of absolute orbit errors of up to 2 km using only two orbits of bearing angle measurements in a wide range of orbit regimes. Additionally, the computation time required to estimate the state of each target with two orbits of measurements is approximately five seconds on a desktop PC with a 3.5GHz processor using the analytical dynamics model. The computation cost increases linearly with the number of targets in the local swarm, allowing the algorithm to efficiently scale to large swarms.

VI. SEQUENTIAL ORBIT DETERMINATION

The SOD module continually refines estimates of the orbits of all spacecraft in the local swarm as well as auxiliary parameters (e.g. sensor biases, ballistic coefficients, and differential clock offsets) by seamlessly fusing measurements from all observers transmitted over the ISL. The SOD module is based on a the UKF, which preserves higher order moments in the probability distribution to enable maneuver-free convergence using angles-only measurements from a single observer [18]. Three additional features are included in the SOD module to to maximize performance using measurements from multiple observers. First, adaptive process noise estimation is used to improve convergence speed and robustness to errors in the dynamics model [31]. Second, the state definition is organized in a way that exploits the structure of the Cholesky factorization to reduce the number of calls to the orbit propagator by almost a factor of two [32]. Third, measurements from remote observers are assigned to tracked targets using selection criteria based on the Mahalanobis distances between the estimated bearing angles to each target and each candidate measurement. Let σ_{jk} denote the Mahalanobis distance between the jth measurement from the remote observer and the predicted measurement to the kth target tracked by the local observer (which accounts for all relevant state uncertainties). To minimize erroneous assignments, the jth measurement from the remote observer is assigned to the kth target if three conditions are satisfied:

Condition 1) $\sigma_{jk} \leq \varepsilon_{assign}$
Condition 2) $\sigma_{lk} \geq \varepsilon_{ambig}\ \forall l \neq j$
Condition 3) $\sigma_{jp} \geq \varepsilon_{ambig}\ \forall p \neq k$

where ε_{assign} and ε_{ambig} are user-specified parameters that satisfy $\varepsilon_{ambig} > \varepsilon_{assign} > 0$. These conditions ensure 1) the measurement is close to the modeled measurement to the target using the current state estimate, 2) there is no other candidate measurement that fits the estimated state of the target, and 3) there is no other target with a state estimate that fits the measurement. Figure 4 includes conceptual illustrations of four possible cases of modeled and observed measurements from a remote observer which (from left to right) show all conditions satisfied and violations of Condition 1, Condition 2, and Condition 3, respectively. Together, these conditions ensure that measurements are only assigned when the observed and modeled measurements uniquely agree with a statistical certainty determined by the values of ε_{assign} and ε_{ambig}. The values of these parameters should be selected

based on the expected number of targets, relative motion geometry, sensor noise, and available orbit knowledge for general swarming missions. However, for scenarios similar to those presented in the following section, the authors have found that setting $\varepsilon_{assign} = 3$ and $\varepsilon_{ambig} = 6$ provide robust measurement assignment performance.

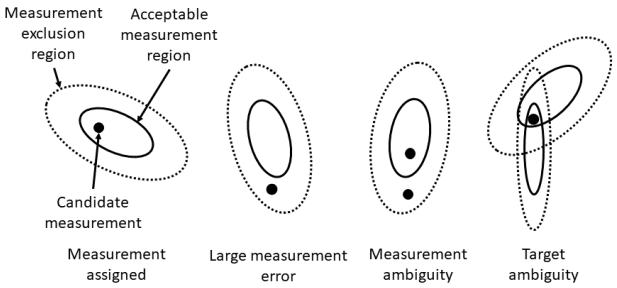

Fig. 4. Illustration of conditions in which all measurement criteria are satisfied (left) and conditions that violate each of the measurement assignment criteria (right).

VII. VALIDATION

The functionality and performance of the payload are validated through hardware-in-the-loop simulation of a challenging scenario that will be part of the upcoming StarFOX experiment. The selected test case includes four spacecraft: the observer and three targets, one of which is also a remote observer. The orbit of the observer and relative orbits of the three targets at the start of the simulation are provided in Table I. The relative orbits for this simulation were selected to be representative of the Starling mission when the formation is deployed in passive safety ellipses, which are known to provide better observability using angles-only measurements [17]. The observer's sensor is pointed in the flight direction throughout the simulation to ensure that all three targets are always visible. Target 3 was selected as the remote observer because it can see all three other spacecraft with a single sensor pointed in the anti-flight direction. An overview of the absolute and relative motion of this formation along with the selected sensor orientation is shown in Figure 5.

TABLE I
INITIAL ABSOLUTE AND RELATIVE ORBITS FOR SIMULATION.

		Absolute orbit				
-	a (km)	$e_x(-)$	$e_y(-)$	$i^{(o)}$	Ω	$u^{(o)}$
Observer	6978	0.0014	0.0014	98	40	105
		Relative orbits				
ROE (m)	$a\delta a$	$a\delta\lambda$	$a\delta e_x$	$a\delta e_y$	$a\delta i_x$	$a\delta i_y$
Target 1	0.0	65000	0	3000	0	3000
Target 2	0.0	133000	0	2600	0	2600
Target 3	0.0	200000	0	1200	0	1200

The ARTMS operations sequence for this simulation is described in the following. First, each observer is provided with an estimate of its position and velocity at a single epoch with 1-σ errors of 10 m and 0.01 m/s per axis, which is

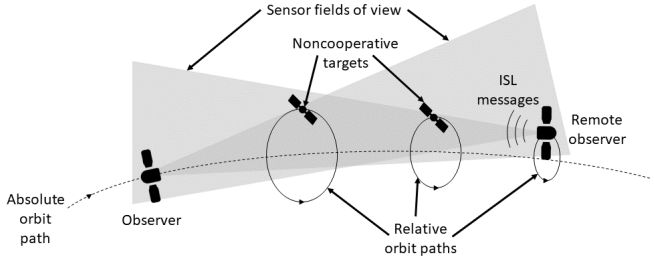

Fig. 5. Illustration of orbits of observers, targets, and sensor orientations in validation simulation.

consistent with estimates provided by GNSS receivers or the Deep Space Network. These estimates enable proper orientation of the sensor on each observer and allow the IMP modules to begin detecting and tracking targets. After three hours (two orbits), the BOD module on each observer is called on each observer to compute refined estimates of its absolute orbit and the relative orbits of all targets detected by the onboard sensor. Once this estimate is computed, the SOD modules on each observer continuously refine the swarm state estimates using measurements form both observers exchanged over the ISL.

The procedure used to compute the simulation inputs and the ground truth data (which is used to assess navigation performance) is as follows. First, the ground truth data is computed by propagating the orbits of each observer and target for 24 hours using a high-fidelity numerical orbit propagator including all substantial perturbations in earth orbit (geopotential, atmospheric drag, solar radiation pressure, and lunisolar third body gravity) [33]. The ground truth data is used to synthesize images of background stars and the other spacecraft as seen by each observer. These synthetic images are then rendered on the display in the Space Rendezvous Laboratory's OS testbed [19]. The display is then imaged by a Blue Canyon Technologies Nano Star Tracker [5], producing the images that are provided to the ARTMS payload for each obserrver. An example image collected by the sensor is shown in Figure 6 along with identifications of stars, targets, and unidentified non-stellar objects. The initial position and velocity estimates for each observer are computed by corrupting the ground truth initial orbits values with zero-mean Gaussian noise with the aforementioned distribution.

The formal covariance (shaded) and estimation errors (lines) for the SOD module of the observer (as specified in Table I) over the course of the simulation are shown in Figure 7. The estimation errors of the absolute and relative orbits are converted to errors in position and velocity in the RTN frame to provide a simple geometric interpretation of the navigation accuracy. The plots start at the 3hr mark when the SOD module is initialized with the estimate from the BOD module, which is subject to errors of a few kilometers. The plots on the left side indicate the difference between the estimated position and velocity of the observer and the

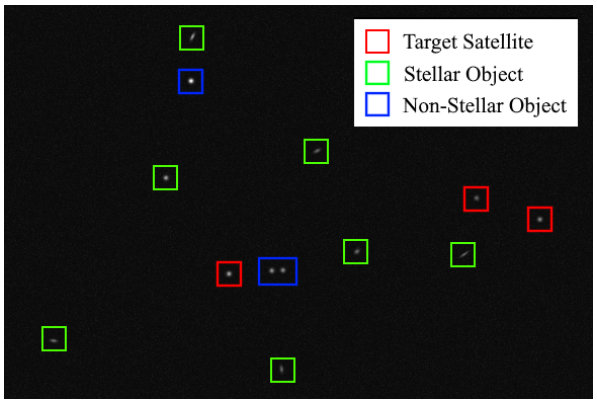

Fig. 6. An example image from the star tracker and OS with IMP classifications.

ground truth value. It is evident that the estimate converges to steady state position errors of under 1 km and velocity errors of less than 0.5 m/s within twelve hours. Additionally, the formal covariance is consistent with the estimation error throughout the simulation. The estimation errors for the relative position and velocity of each target in the RTN (shown in the right plots) also converge to steady state error within twelve hours The steady-state errors in the along-track separations to each target are under 100m and the radial and normal relative position errors are less than 10m. The steady-state relative velocity errors do not exceed 1 cm/s.

Because the relative position and velocity errors include combinations of errors in estimated state parameters, key steady-state error metrics in the absolute and relative orbits are provided in the following. First, the steady state error in the semimajor axis of the absolute orbit is only 34m, which is more than an order of magnitude less than the observed 1 km absolute position error. Second, the steady state formal covariance and estimation error for $a\delta\lambda$ for each target are less than 0.5% of the true separation. The errors in the other ROE (scaled by a for comparison purposes) are less than 0.1m per kilometer of separation.

Overall, these results show that the ARTMS payload provides sufficient navigation accuracy for a wide range of science missions in deep space as well as space situational awareness applications in earth orbit with minimal reliance on a-priori information and translational maneuvers.

VIII. CONCLUSIONS

This paper presented an overview of the Absolute and Relative Trajectory Measurement System (ARTMS), which is a software payload that provides autonomous, distributed, and scalable navigation for spacecraft swarms in deep space using inexpensive optical sensors. The payload consists of three modules: image processing, batch orbit determination, and sequential orbit determination. Image processing provides batches of measurements to each observed target using time-tagged images from the onboard camera and a single coarse estimate of the observer's orbit. The batch orbit determination module uses the estimate of the observer's orbit and batches of bearing angles to each target to provide estimates of the orbits of each spacecraft or resident space object in the local swarm. Finally, the sequential orbit determination module estimates the orbits of the local swarm as well as auxiliary parameters such as ballistic coefficients or differential clock offsets by seamlessly fusing measurements from multiple observers received over the inter-satellite link in an unscented Kalman filter.

The functionality and performance of the payload were demonstrated through a first-of-a-kind sensor-in-the-loop simulation of autonomous angles-only navigation using two cooperative observers. In this simulation, each observer is only provided with a single estimate of its orbit, images from the onboard sensor, and measurements from a remote observer transmitted over the inter-satellite link. It is found that the payload is able to initialize the sequential filter with range errors of only a few kilometers after two orbits and converge to steady state within ten hours. The system provides navigation solutions with steady state absolute position and velocity errors of better than 1 km and 0.5 m/s, range errors of better than 250 m, and estimates of other relative orbital elements with errors no larger than 0.1m per kilometer of separation. These results show that the ARTMS payload provides accurate, robust, and scalable navigation capability for spacecraft swarms with minimal reliance on a-priori information, meeting a critical need for future deep-space science and space situational awareness missions.

ACKNOWLEDGMENT

The authors would like to acknowledge the contributions of Toby Bell to the development of the ARTMS software modules.

REFERENCES

[1] B. D. Tapley, S. Bettadpur, M. Watkins, and C. Reigber, "The Gravity Recovery and Climate Experiment: Mission Overview and Early Results," *Geophysical Research Letters*, Vol. 31, No. 9, 2004.

[2] G. Krieger, A. Moreira, H. Fiedler, I. Hajnsek, M. Werner, M. Younis, and M. Zink, "TanDEM-X: A Satellite Formation for High-Resolution SAR Interferometry," *IEEE Transactions on Geoscience and Remote Sensing*, Vol. 45, No. 11, 2007, pp. 3317–3341.

[3] S. D'Amico, J.-S. Ardaens, and R. Larsson, "Spaceborne Autonomous Formation-Flying Experiment on the PRISMA Mission," *Journal of Guidance, Control, and Dynamics*, Vol. 35, May 2012, pp. 834–850, DOI:10.2514/1.55638.

[4] J. Burch, T. Moore, R. Torbert, and B. Giles, "Magnetospheric Multiscale Overview and Science Objectives," *Space Science Reviews*, Vol. 199, No. 1-4, 2016, pp. 5–21.

[5] S. Palo, G. Stafford, and A. Hoskins, "An Agile Multi-Use Nano Star Camera for Constellation Applications," *Proceedings of the Small Satellite Conference, Advanced Technologies II, SSC13-III-5*, 2013.

[6] S. D'Amico, J.-S. Ardaens, G. Gaias, H. Benninghoff, B. Schlepp, and J. L. Jørgensen, "Noncooperative Rendezvous Using Angles-Only Optical Navigation: System Design and Flight Results," *Journal of Guidance, Control, and Dynamics*, Vol. 36, Nov. 2013, pp. 1576–1595, DOI:10.2514/1.59236.

[7] G. Gaias, J.-S. Ardaens, and S. D'Amico, "The Autonomous Vision Approach Navigation and Target Identification (AVANTI) Experiment: Objectives and Design," *9th International ESA Conference on Guidance, Navigation & Control Systems, Porto, Portugal*, 2014.

[8] G. Gaias and J.-S. Ardaens, "Flight Demonstration of Autonomous Noncooperative Rendezvous in Low Earth Orbit," *Journal of Guidance, Control, and Dynamics*, Vol. 41, No. 6, 2017, pp. 1337–1354.

[9] J.-S. Ardaens and G. Gaias, "Angles-Only Relative Orbit determination in Low Earth Orbit," *Advances in Space Research*, Vol. 61, No. 11, 2018, pp. 2740–2760.

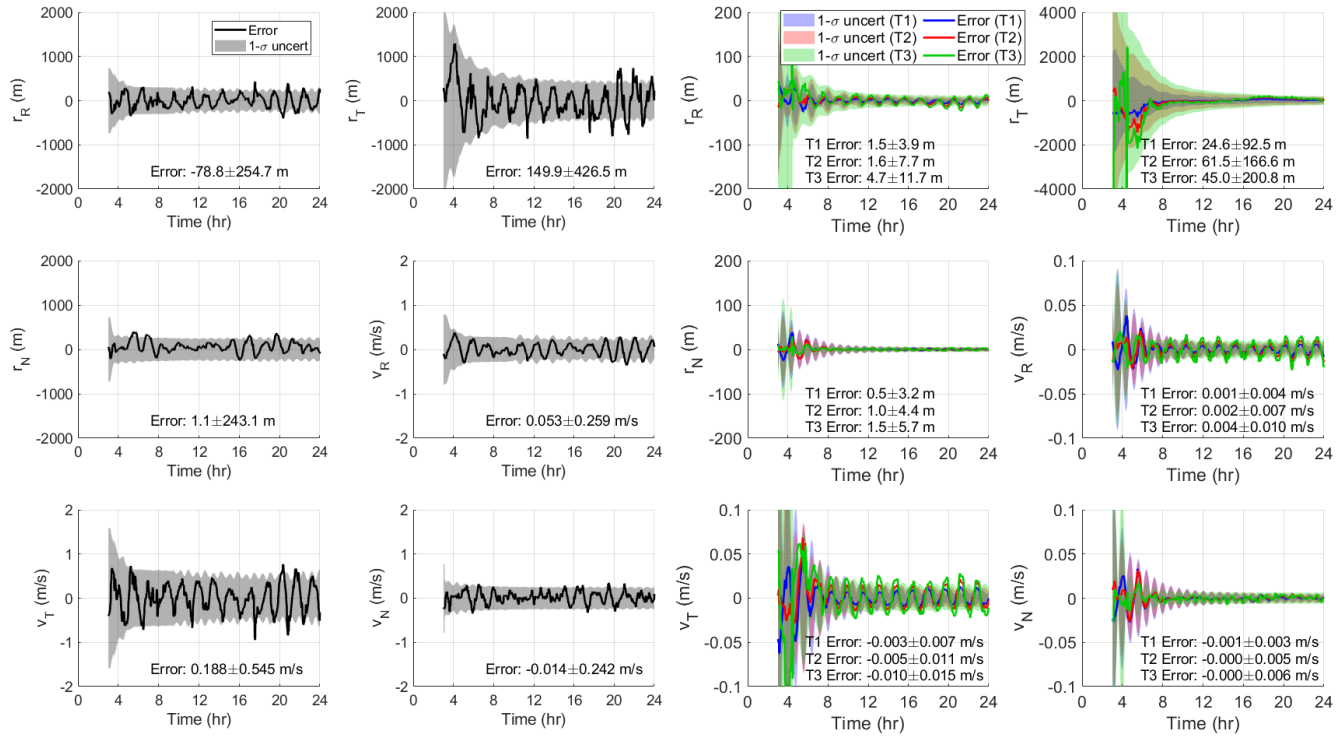

Fig. 7. Estimation errors (lines) and formal covariance (shaded) for absolute orbit (left) and relative orbits of Target 1 (blue), Target 2 (red), and Target 3 (green) converted to position and velocity in the radial/tangential/normal (RTN) frame including steady state error values.

[10] B. Vo, M. Mallick, Y. Bar-shalom, S. Coraluppi, R. Osborne, R. Mahler, and B. Vo, "Multitarget Tracking," *Wiley Encyclopedia of Electrical and Electronics Engineering*, Springer International Publishing, 2015.

[11] S. K. Garg, "Initial Relative Orbit Determination Using Second-Order Dynamics and Line-of-Sight Measurements," Master's thesis, Auburn University, 2015.

[12] J.-S. Ardaens and G. Gaias, "A numerical approach to the problem of angles-only initial relative orbit determination in low earth orbit," *Advances in Space Research*, Vol. 63, No. 12, 2019, pp. 3884–3899.

[13] Y. Hu, I. Sharf, and L. Chen, "Three-Spacecraft Autonomous Orbit Determination and Observability Analysis with Inertial Angles-Only Measurements," *Acta Astronautica*, Vol. 170, 2020, pp. 106–121.

[14] J. Sullivan, *Nonlinear Angles-Only Orbit Estimation for Autonomous Distributed Space Systems*. PhD thesis, Stanford University, 2020.

[15] H. Sanchez, D. McIntosh, H. Cannon, C. Pires, M. Field, J. Sullivan, S. D'Amico, L. Mall, and B. O'Connor, "Starling-1: Swarm Technology Demonstration," *32nd Annual Small Satellite Conference*, Logan, UT, Aug. 2018.

[16] J. Kruger and S. D'Amico, "Autonomous Angles-Only Multitarget Tracking for Spacecraft Swarms," *2020 AAS/AIAA Astrodynamics Specialist Conference*, Lake Tahoe, California, 2020.

[17] A. W. Koenig and S. D'Amico, "Observability-Aware Numerical Algorithm for Angles-Only Initial Relative Orbit Determination," *2020 AAS/AIAA Astrodynamics Specialist Conference*, Lake Tahoe, California, 2020.

[18] J. Sullivan, A. W. Koenig, J. Kruger, and S. D'Amico, "Generalized Angles-Only Navigation Architecture for Autonomous Distributed Space Systems," *Journal of Guidance, Control, and Dynamics*, 2020. Submitted.

[19] C. Beierle and S. D'Amico, "Variable Magnification Optical Stimulator for Training and Validation of Spaceborne Vision-Based Navigation," *Journal of Spacecraft and Rockets*, Vol. 56, No. 4, 2019.

[20] D. C. Woffinden and D. K. Geller, "Observability Criteria for Angles-Only Navigation," *IEEE Transactions on Aerospace and Electronic Systems*, Vol. 45, No. 3, 2009, pp. 1194–1208.

[21] S. D'Amico, *Autonomous Formation Flying in Low Earth Orbit*. PhD Thesis, Delft University, 2010. OCLC: 839641932.

[22] A. W. Koenig, T. Guffanti, and S. D'Amico, "New State Transition Matrices for Relative Motion of Spacecraft Formations in Perturbed Orbits," *Journal of Guidance, Control, and Dynamics*, Sept. 2016, DOI:10.2514/6.2016-5635.

[23] T. Guffanti, S. D'Amico, and M. Lavagna, "Long-Term Analytical Propagation of Satellite Relative Motion in Perturbed Orbits," *27th AAS/AIAA Space Flight Mechanics Meeting*, San Antonio, TX, 2017.

[24] J. Sullivan, T. A. Lovell, and S. D'Amico, "Angles-Only Navigation for Autonomous On-Orbit Space Situational Awareness Applications," *AAS/AIAA Astrodynamics Specialist Conference, Snowbird, UT*, 2018.

[25] D. Mortari, M. A. Samaan, C. Bruccoleri, and J. L. Junkins, "The pyramid star identification technique," *Navigation*, Vol. 51, No. 3, 2004, pp. 171–183.

[26] J. R. Wertz, *Spacecraft Attitude Determination and Control*. Springer Science & Business Media, 2012.

[27] J. Kruger and S. D'Amico, "Autonomous Angles-Only Multi-Target Tracking for Spacecraft Swarms," *IEEE Transactions on Aerospace and Electronic Systems*, 2020. Submitted.

[28] S. Blackman, "Multiple Hypothesis Tracking For Multiple Target Tracking," *IEEE Aerospace and Electronic Systems Magazine*, Vol. 19, No. 1, 2004, pp. 5–18.

[29] J. Sullivan and S. D'Amico, "Nonlinear Kalman Filtering for Improved Angles-Only Navigation Using Relative Orbital Elements," *Journal of Guidance, Control, and Dynamics*, July 2017, pp. 1–18, DOI:10.2514/1.G002719.

[30] M. Ester, H.-P. Kriegel, J. Sander, and X. Xu, "A Density-Based Algorithm for Discovering Clusters a Density-Based Algorithm for Discovering Clusters in Large Spatial Databases with Noise," *Proceedings of the Second International Conference on Knowledge Discovery and Data Mining*, AAAI Press, 1996, p. 226–231.

[31] J. Sullivan and S. D'Amico, "Adaptive Filtering for Maneuver-Free Angles-Only Navigation in Eccentric Orbits," San Antonio, Texas, 2017.

[32] N. Stacey and S. D'Amico, "Adaptive and Dynamically Constrained Process Noise Estimation for Orbit Determination," *2019 AAS/AIAA Astrodynamics Specialist Conference*, Portland, Maine, 2019.

[33] V. Giralo and S. D'Amico, "Development of the Stanford GNSS Navigation Testbed for Distributed Space Systems," *Institute of Navigation, International Technical Meeting*, 2018.